

# Bistable twisted-bend and twisted-nematic liquid crystal display

Y. W. Li<sup>a)</sup> and H. S. Kwok

Center for Display Research, Hong Kong University of Science and Technology, Clear Water Bay, Hong Kong

(Received 29 July 2009; accepted 30 September 2009; published online 5 November 2009)

Bistability of twisted-bend and twisted configuration is found. It is based on the elastic and topological inequivalency of director orientation. Multiple states of minimum local energy exist, with appropriate boundary conditions. The effects of elastic constants,  $d/P$  ratio and pretilt angle are also investigated. Fast electrical switching time  $<500 \mu\text{s}$  and high average contrast of 45:1 are obtained experimentally. © 2009 American Institute of Physics. [doi:10.1063/1.3254212]

One important class of liquid crystal displays is those with permanent memory. The display can be in either of two stable states without any voltage bias. A zero power display as this, is attractive for many applications. There are several types of bistable nematic liquid crystal displays, such as bistable bend splay display (BBS), bistable twisted nematic display (BTN). Bistability of a nematic layer may be realized by various means. For instance, the stable states may differ in the azimuthal of the preferred molecule orientation. These two azimuths correspond to the directions of easy orientation on each of the specially prepared substrates. Bistable orientations interswitching is based on the surface anchoring energy breaking. An example is the BTN. Durand *et al.*,<sup>1</sup> demonstrated a variant of the BTN bistable twisted nematic display where the bistable twist states are  $0^\circ$  and  $180^\circ$ . In this case, strong asymmetric polar anchoring and thin cell gaps,  $1.5 \mu\text{m}$ , have to be used. Stalder and Schadt<sup>2</sup> proposed stabilizing the BTN device by domains with bias tilt patterned substrate. Kwok *et al.*,<sup>3,4</sup> generalized the bistable twist states to  $\phi$  and  $\phi+\pi$  twist states, where  $\phi$  can be one of several published values. Another example of bistable nematic display is based on topological bistability of the director at polar orientation. Yu and Kwok<sup>5</sup> suggested a BBS display using high tilt angle at the top and bottom boundaries. The switching between these states required interdigital electrode structure or making use of the dual frequency liquid crystal.<sup>6</sup>

From the previously mentioned nematic bistable liquid crystal display, it is found that they are based on the topological in-equivalency, they are separated by sufficiently high energy barrier or  $\pi$ -wall.<sup>7,8</sup> These bistable devices are classified to either (twist, twist) or (bend, splay) groups. Here, we show yet another new bistable display device. It consists of two bistable states, twisted-bend (TB), and twisted-nematic (T) states. Such device is called BBT display, which clearly is classified into none of the bistable groups mentioned above. In this paper, bistability of BBT under the effects of  $d/P$  ratio, pretilt angle and Frank elastic constants will be presented.

The simplest description of deformations within liquid crystals may be obtained at the elastic level only. By considering spatial variations of the director of the nematic liquid crystal (NLC)  $\mathbf{n}$  and the need to conserve the symmetry of  $n=-n$ , a free energy can be described by Frank free energy density,<sup>9</sup>

$$F = \frac{1}{2}[K_{11}(\nabla \cdot \mathbf{n})^2 + K_{22}(\mathbf{n} \cdot \nabla \times \mathbf{n} - q_0)^2 + K_{33}|\mathbf{n} \times \nabla \times \mathbf{n}|^2], \quad (1)$$

where  $K_{11}$ ,  $K_{22}$ , and  $K_{33}$  are the splay, twist, and bend elastic constants, respectively,  $q_0$  is the intrinsic twist of the liquid crystal layer, and  $\mathbf{n}=(\cos \phi \cos \theta \sin \phi \cos \theta \sin \theta)$ . The minimization of the total energy leads to the usual Euler-

Lagrange (EL) equations  $(\partial F)/(\partial \theta)=(d \partial F / \partial \theta) / (dz)$  and  $(\partial F)/(\partial \phi)=(d \partial F / \partial \phi) / (dz)$  subjected to the top and bottom boundary conditions. The solution of director orientation  $\theta(z)$  and  $\phi(z)$  are sought by the numerical solutions of such second order nonlinear equation.

The deformation of TB and T states are depicted in Fig. 1 based on the solution obtained by Eq. (1) with parameters  $K_{11}=2 \text{ pN}$ ,  $K_{22}=2 \text{ pN}$ , and  $K_{33}=10 \text{ pN}$ , the cell gap  $d=5 \mu\text{m}$  and cell gap to pitch ratio  $d/P=1.125$ . By increasing  $d/P$ , the total elastic energy for the TB and the T deformation increases at different rates and finally come across at a certain equilibrium point. At the equilibrium situation, both deformations will have the same total elastic energy are governed by same boundary conditions of  $\mathbf{A}$  and  $\mathbf{B}$  or  $\mathbf{B}'$ . The two states are quite different as the liquid crystal tilt angle at the middle layer  $\theta_m$  is planar or  $0^\circ$  for the T state and is vertical  $90^\circ$  for the TB state. To depict the configuration of the TB and T states in a more instructive way, the unit sphere representation<sup>10</sup> can be applied as shown in Fig. 2. The director alignment at any point along  $z$  direction between the two substrates is described in spherical coordinates by tilt angle  $\theta$  and azimuthal angle  $\phi$ . In other words, they are

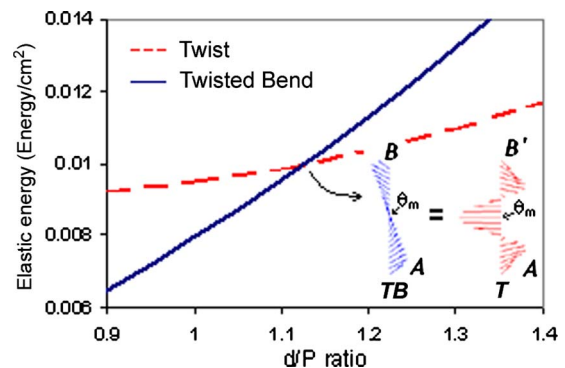


FIG. 1. (Color online)  $d/P$  ratio effect on free elastic energy of TB and T deformation.

<sup>a)</sup>Electronic mail: eetank@ust.hk.

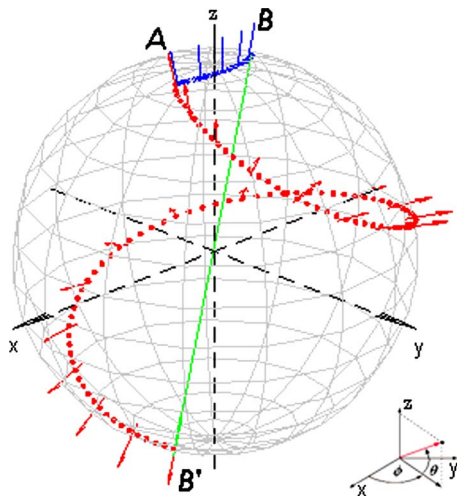


FIG. 2. (Color online) Unit sphere representation for TB and T deformation.

represented as a point  $(\theta, \phi)$  on the surface of the unit sphere in Fig. 2. Due to the symmetry of NLC director, any direction, i.e.,  $\mathbf{B}$ , on the sphere  $(\theta, \phi)$  is equivalent to opposite direction, i.e.,  $\mathbf{B}'$ ,  $(-\theta, \phi)$ . This unit sphere is a very useful tool to illustrate the topological difference between two states that cannot change continuously from one, i.e.,  $\mathbf{AB}$  to the other i.e.,  $\mathbf{AB}'$ , even though they have identical physical boundary conditions. Such feature is the core idea of bistable display.<sup>7,8</sup> Figure 2 shows the boundary conditions  $\mathbf{A}(\theta_0, 0)$  and  $\mathbf{B}(\theta_0, \pi)$  where  $\theta_0 = 75^\circ$ . The boundary condition  $\mathbf{B}'(-\theta_0, 2\pi)$  is actually equivalent to  $\mathbf{B}$ . Hence, on the unit sphere, there are two traces  $\mathbf{AB}$  and  $\mathbf{AB}'$  which satisfy the same boundary conditions and are possible solutions of the EL equation.

It is clear that TB deformation  $\mathbf{AB}$  (blue line) is not able to transform to twisted deformation (red dot line) described by  $\mathbf{AB}'$  in a continuous way, but must overcome a discontinuous  $\pi$  jump (green line) of the director from  $\mathbf{B}$  to  $\mathbf{B}'$ . Furthermore, the paths (deformation) of twisted bend ( $\mathbf{AB}$ ) and twisted states ( $\mathbf{AB}'$ ) are unique pairs. This is because their total elastic energy is the same. Therefore, the TB and the T deformation is a truly bistable deformation. Heuristically, it can be seen that  $\mathbf{AB}$  is not purely a bend state. Owing to the effect of the chiral dopant, the tilted angle in middle layer of deformation  $\theta_m$  is not perfectly upright at  $90^\circ$ . Maximum  $\theta_m$  is about  $\approx 86^\circ$ . However, from an optical performance point of view, twist sense at such high  $\theta_m$ , which is very close to  $90^\circ$ , is physically meaningless. The optical performance is dominated by the bend effect.

From the previous EL model studies, the stability of the BBT mode is governed by several parameters:  $K$  elastic constants,  $d/P$  ratio and pretilt angles. According to the unit sphere shown in Fig. 2, there are infinite pairs of bistable deformations under different boundary condition ( $\mathbf{A}$ ,  $\mathbf{B}$ , and  $\mathbf{B}'$ ) theoretically. To investigate the effect of pretilt angles and  $d/P$  ratio, the other parameters of liquid crystal are fixed as  $K_{11} = 2$  pN,  $K_{22} = 2$  pN,  $K_{33} = 10$  pN, and cell gap  $d = 5$   $\mu\text{m}$ . Figure 3(a) shows that as the pretilt angles increase, the tilt angle  $\theta_m$  at the middle layer of liquid crystal deformation exhibits a sharp jump (dash line) from  $20^\circ$  up to  $70^\circ$ . Therefore, the pretilt angles should be as high as  $73^\circ$  in order to obtain the TB deformation. The sharp jump induces deformation transition from  $\pi$ -twisted splay to twisted bend de-

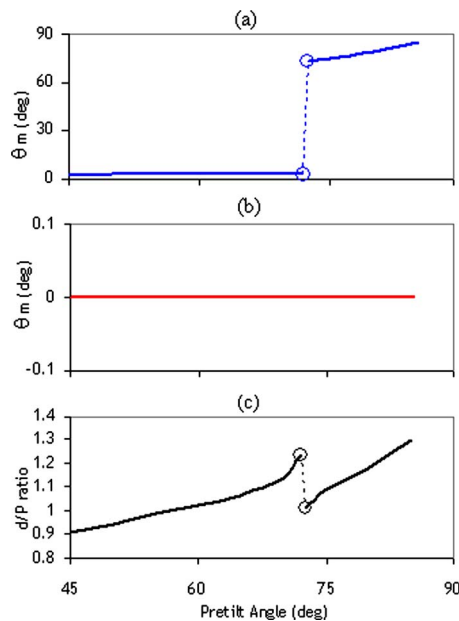


FIG. 3. (Color online)  $\theta_m$  for (a) TB and (b) T deformation under different pretilt angles, and (c) shows the corresponding  $d/P$  ratio.

formation. Figure 3(b) shows the tilt angle  $\theta_m$  of the corresponding  $2\pi$  twisted deformation ( $\mathbf{AB}'$ ). The tilt angles  $\theta_m$  are always maintained at  $0^\circ$  under different pretilt angle boundary conditions. These results coincide with the predictions shown on the unit sphere in Fig. 2. Figure 3(a) shows the dependence of  $\theta_m$  on the pretilt angle for curve  $\mathbf{AB}$  (TB mode) and Fig. 3(b) shows that for curve  $\mathbf{AB}'$  (T mode). Figure 3(c) shows the corresponding  $d/P$  ratio. It can be seen that as the pretilt angle increases, the required  $d/P$  ratio also increases. This is because the bend effect became more favorable as the pretilt angle increased; larger  $d/P$  ratio is required to balance the elastic energy for the TB and T states. From Figs. 3(a)–3(c), we found that if the pretilt angle is high enough, there is always a suitable  $d/P$  ratio to produce bistability of the TB and the T deformations.

To confirm the above idea, a BBT device is fabricated. The alignment surface is made of spin coating a mixture of vertical polyimide JALS-2021 and horizontal polyimide JALS-9203.<sup>11</sup> By carefully controlling the conditions of curing, an alignment layer with nanotexture surface with H and V domain are formed. Such nanotexture polyimide surface induces  $85^\circ$  pretilt angle with applied liquid crystal MLC-2048 from Merck. The elastic constants of applied NLC are  $K_{11} = 12.4$  pN,  $K_{22} = 10.1$  pN,  $K_{33} = 24.7$  pN. The optical an-

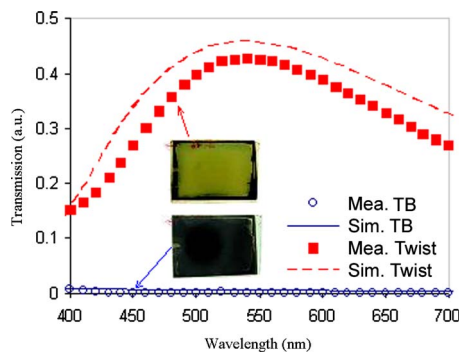


FIG. 4. (Color online) Measured and simulated transmission spectrum of the sample.

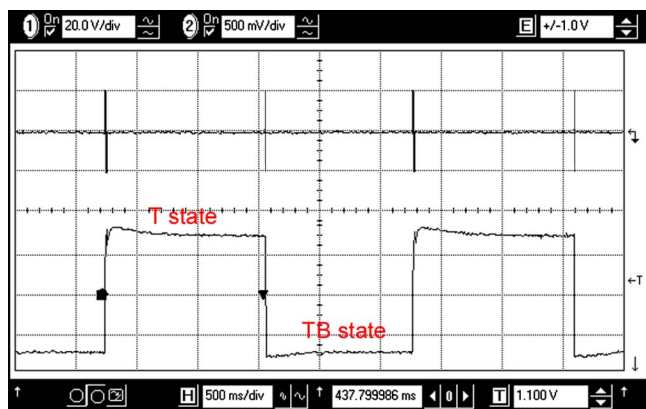


FIG. 5. (Color online) Optical response of BBT, upper line is driving signal, lower line is optical response.

isotropy is  $\Delta n=0.22$ ,  $n_e=1.7$ . The dielectric anisotropy  $\Delta\epsilon$  is  $+3.0$  at 1 kHz driving signal and  $-2.8$  at 50 kHz. The cross-over frequency at room temperature is about 18 kHz.<sup>11</sup> The top and bottom alignment substrates are separated by  $5\ \mu\text{m}$  spherical spacers. 1.5% by weight of S811 chiral dopant is added into MLC-2048. The expected  $d/P$  ratio is 1.17. The polarizer and analyzer are  $\pm 45^\circ$  to the input director of NLC.<sup>12</sup> The transmission spectrums of T and TB deformation are simulated by standard Jones matrix approaches.<sup>13,14</sup> Figure 4 shows the transmission spectrum measured and the simulated results. It can be seen that they are in good agreement. The average contrast ratio is 45:1. This experiment also confirmed the correctness of fabrication and the simulation model. Owing to the dual frequency property of MLC-2048, the interstate switching can be easily obtained by applying a different frequency signal. If the device is driven at 1 kHz, MLC-2048 behaves like positive liquid crystal, T  $\rightarrow$  TB switching occurs. On the other hand, when a 50 kHz signal is applied, TB  $\rightarrow$  T switching is effected. The switching dynamic is presented in Fig. 5. The upper and lower lines

are driving signal and optical response of the BBT respectively. The T  $\rightarrow$  TB switching requires 1 kHz 20 V electrical driving pulse for 500  $\mu\text{s}$  and the corresponding optical response time is 3.1 ms. Owing to the backflow effect, the TB-T optical response time is 7.4 ms, twice as long as T-TB. It also requires 5 ms 20 V 50 kHz electrical pulse to induce such switching.

In conclusion, the bistability of the TB and the twisted deformation is found. The effects of elastic constants,  $d/P$  ratio and pretilt angle on the bistability are studied theoretically. The BBT device is fabricated and where fast electrical switching time  $<500\ \mu\text{s}$  and high average contrast 45 are obtained. Such optical and electrical performance makes such device becoming strong competitive candidates of the zero power display device.

This research was sponsored by the Hong Kong Government Research Grants Council Grant No. 614408. The authors also thank Dr. Anatoli Muravski for some of the measurements.

<sup>1</sup>I. Dozov, M. Nobili, and G. Durand, *Appl. Phys. Lett.* **70**, 1179 (1997).

<sup>2</sup>M. Stalder and M. Schadt, *Liq. Cryst.* **30**, 285 (2003).

<sup>3</sup>T. Z. Qian, Z. L. Xie, H. S. Kwok, and P. Sheng, *Appl. Phys. Lett.* **71**, 596 (1997).

<sup>4</sup>Z. L. Xie and H. S. Kwok, *J. Appl. Phys.* **84**, 77 (1998).

<sup>5</sup>X. J. Yu and H. S. Kwok, *Appl. Phys. Lett.* **85**, 3711 (2004).

<sup>6</sup>F. S. Y. Yeung, Y. W. Li and H.-S. Kwok, *SID Int. Symp. Digest Tech. Papers* **36**, 1770 (2005).

<sup>7</sup>J. Cheng and R. N. Thurston, *J. Appl. Phys.* **52**, 2756 (1981).

<sup>8</sup>G. D. Boyd, J. Cheng, and P. D. T. Ngo, *Appl. Phys. Lett.* **36**, 556 (1980).

<sup>9</sup>F. C. Frank, *Discuss. Faraday Soc.* **25**, 19 (1958).

<sup>10</sup>G. Porte, *J. Phys.* **38**, 509 (1977).

<sup>11</sup>F. S. Y. Yeung, Y. J. Ho, Y. W. Li, F. C. Xie, O. Tsui, P. Sheng, and H. S. Kwok, *Appl. Phys. Lett.* **88**, 051910 (2006).

<sup>12</sup>F. S. Y. Yeung, Y. W. Li, and H. S. Kwok, *SID Int. Symp. Digest Tech. Papers* **38**, 687 (2006).

<sup>13</sup>A. Lien, *Appl. Phys. Lett.* **57**, 2767 (1990).

<sup>14</sup>F. H. Yu and H. S. Kwok, *J. Opt. Soc. Am. A Opt. Image Sci. Vis* **16**, 2772 (1999).